

# How Do Low-Energy (0.1–2 eV) Electrons Cause DNA-Strand Breaks?

JACK SIMONS\*

Chemistry Department, University of Utah,  
Salt Lake City, Utah 84112

Received March 24, 2006

## ABSTRACT

We overview our recent theoretical predictions and the innovative experimental findings that inspired us concerning the mechanisms by which very low-energy (0.1–2 eV) free electrons attach to DNA and cause strong (ca. 4 eV) covalent bonds to break causing so-called single-strand breaks. Our primary conclusions are that (i) attachment of electrons in the above energy range to base  $\pi^*$  orbitals is more likely than attachment elsewhere and (ii) attachment to base  $\pi^*$  orbitals most likely results in cleavage of sugar–phosphate C–O  $\sigma$  bonds. Later experimental findings that confirmed our predictions about the nature of the electron attachment event and about which bonds break when strand breaks form are also discussed. The proposed mechanism of strand break formation by low-energy electrons involves an interesting through-bond electron-transfer process.

## 1. Introduction

Ionizing radiation can damage DNA several ways,<sup>1</sup> but it is primarily through secondary reactions involving species generated in an initial ionization event that damage occurs. Water can be ionized to generate electrons, OH, or H radicals, which can then attack DNA and cleave chemical bonds. Alternatively, components of DNA itself can be ionized by the radiation to produce radical cations and electrons. The free electrons generated when water or DNA is ionized have a wide range of energies (1–20 eV), but they lose energy through collisions and can eventually yield solvated electrons. As these free electrons reach energies near the ionization thresholds of water or components of DNA (ca. 7–8 eV), they can further ionize either water or DNA, generating more reactive species and thus more potential for damage.

However, once the electrons reach energies below 7–8 eV, they can no longer produce secondary ionizations. Nevertheless and perhaps surprisingly, it is still possible for electrons having kinetic energies even as low as 0.1 eV to damage DNA, and it is such processes upon which

Jack Simons was born April 2, 1945 in Youngstown, OH, and he attended primary and secondary school in nearby Girard, OH. After he earned a B.S. degree in chemistry from the Case Institute of Technology in 1967, he held an NSF Graduate Fellowship at the University of Wisconsin, Madison, WI, where he earned his Ph.D. in 1970 under Prof. J. E. Harriman. He then was an NSF Postdoctoral Fellow at MIT, where he worked with Prof. J. M. Deutch. In 1971, he joined the University of Utah faculty, where he now holds the position of Henry Eyring Scientist and Professor of Chemistry. The author of over 300 papers and 6 books and the advisor to more than 60 Ph.D. and postdoctoral students, he has held Sloan, Dreyfus, and Guggenheim Fellowships. His research is focused on the theoretical study of electron–molecule interactions and molecular anions. He has written and maintains a web site (<http://simons.hec.utah.edu/TheoryPage>) on theoretical chemistry for students and nonexperts.

the present Account is focused. The keys to understanding how such low-energy electrons can induce covalent-bond cleavage in DNA lie (a) in the energies and nodal characters of the low-energy unfilled molecular orbitals of DNA, (b) in the mechanism by which electrons attach to these orbitals, (c) in a through-bond electron-transfer process, and (d) in identifying the bond most susceptible to electron-induced cleavage.

Most readers would likely be able to predict that it is the DNA base  $\pi^*$  or phosphate P=O  $\pi^*$  orbitals that are the lowest energy orbitals into which low-energy electrons might attach. However, the author challenges readers to predict which covalent bond within DNA is the most susceptible to cleavage once such an electron has attached.

The remainder of this Account is organized as follows. We first summarize the recent history of synergistic experimental and theoretical research on damage to DNA by low-energy electrons. In section 2, we discuss the experiments that motivated our work on this problem. In section 3, we address the issue of where (i.e., into which orbital) a low-energy electron most likely attaches to DNA, which bonds are most susceptible to cleavage, and the mechanism by which an electron attaches and subsequently causes bond cleavage. In section 4, we summarize the subsequent experimental findings that verified our theoretical predictions. Finally, section 5 offers a summary of our main findings on this subject.

## 2. The Experiments

Since the year 2002, we have been involved in<sup>2–6</sup> using electronic structure theory to characterize mechanisms by which electrons attach to and subsequently fragment chemical bonds in DNA. Our work in this area was inspired by year 2000 novel experimental findings<sup>7</sup> from the Sanche group in which strand breaks in DNA were produced by electrons having kinetic energies as low as 3 eV. The plasmid *Escherichia coli* DNA samples used in ref 7 were suspended in Nanopure water and subsequently desiccated. As a result, each such sample was very dry (containing only structural water molecules) and possessed counteranions. Thus, the DNA samples were charge-neutral in the regions of their phosphate units. After a sample was irradiated (at room temperature for a fixed time duration) with an electron beam of known current density and known kinetic energy, the DNA sample was subjected to gel electrophoresis analysis. This analysis allowed workers of ref 7 to quantify the amount of sample that had been undamaged, had undergone a single-strand break (SSB), or had realized a double-strand break (DSB).

The yields of SSBs were observed to depend upon the kinetic energy of the incident electron in a manner (see Figure 1) that suggested (because peaks and valleys appeared) some kind of resonant process.

\* To whom correspondence should be addressed. E-mail: [simons@chemistry.utah.edu](mailto:simons@chemistry.utah.edu).

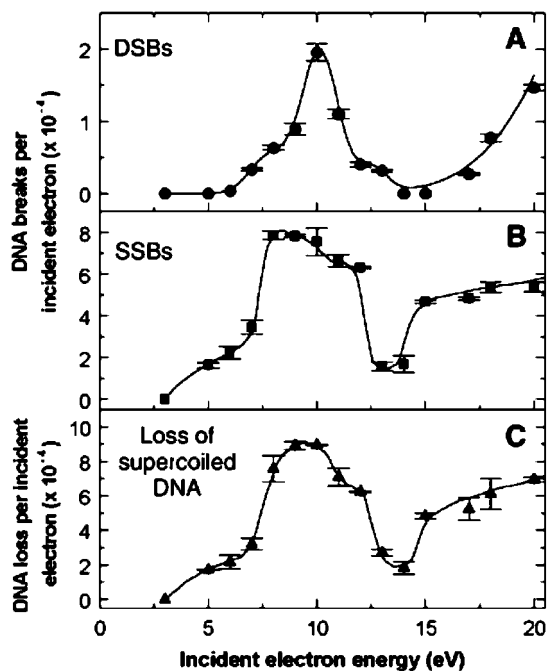


**FIGURE 1.** Yield of SSBs (middle panel) per attached electron as a function of the kinetic energy of the incident electron (Figure 1 of ref 7).

The energies at which the peaks in the SSB plots occurred suggested<sup>7</sup> that the SSB is initiated by electrons attaching to the  $\pi^*$  orbitals of the DNA bases to form so-called core-excited resonance states. These states arise when an electron is captured by an electronically excited state. In the case at hand, an electron attaches to a base  $\pi^*$  orbital and loses energy by simultaneously exciting another electron from a  $\pi$  to a  $\pi^*$  orbital. This can be thought of as involving the following process:  $e^- + \pi^2 \rightarrow \pi^1\pi^{*2}$ .

When the author first read ref 7, he wondered why SSBs were not observed below 3 eV. The Burrow group<sup>8</sup> had shown that electrons of even lower energies attach, with cross-sections near  $1 \text{ \AA}^2$ , to  $\pi^*$  orbitals of the bases of DNA to form so-called shape resonance anions. In contrast to the core-excited resonances in which an electron attaches and excites another electron, in a shape resonance, an electron attaches but no further electronic excitation occurs. Therefore, although the Burrow data indicated that all DNA bases have shape-resonance states lying considerably below (e.g., 0.1–2 eV as shown in Figure 2) the threshold in Figure 1, no SSBs were reported below 3 eV in ref 7. This led us to wonder whether shape resonances were simply too low in energy to cause SSBs. However, we noted that experimental limitations in ref 7 would not allow those experiments to detect strand breaks that might occur below ca. 3 eV. Therefore, we decided to explore whether even lower energy electrons than used in ref 7 could induce strand breaks in DNA by forming shape resonance rather than core-excited resonances.

Before moving on to discuss the series of theoretical studies that we undertook, it is appropriate to mention other recent experimental findings that contributed to the “big picture” analysis of how and where bond cleavages

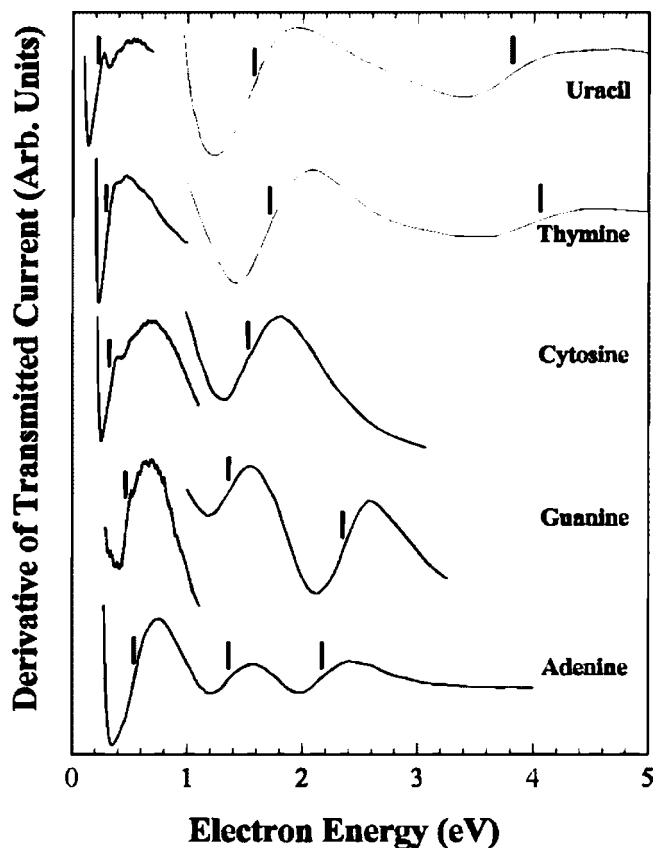


**FIGURE 2.** Electron transmission spectra of the four DNA bases showing the energies (vertical lines) at which the low-energy  $\pi^*$  orbitals occur (Figure 1 of ref 8).

**FIGURE 3.** DNA bases thymine and cytosine showing the  $N_1$  nitrogen atom that bonds to a deoxyribose (sugar) fragment in DNA (and, for thymine, to a sugar in thymidine).

can be induced in DNA by low-energy electrons. Although there have been a large number of experiments involving electrons and DNA fragments, only a fraction of them have used electrons in the energy range of interest in the present work. To retain our focus on energies below ca. 3 eV, we will now discuss primarily the experiments in this energy range that guided our thinking.

In 2005, the Illenberger and Märk groups<sup>9</sup> collaborated to show that all of the bases of DNA can attach electrons at energies below 3 eV and lose a hydrogen atom to produce a base anion:  $B + e^- \rightarrow (B - H)^- + H$ . Moreover, they showed for thymine (see Figure 3) that the loss of an H atom from the  $N_1$  position (the nitrogen bonded to the deoxyribose in DNA) is favored [because of the high

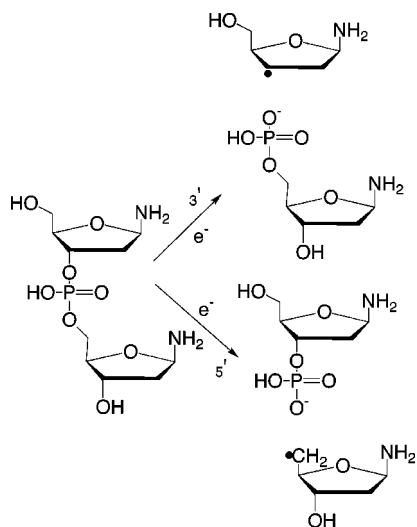


**FIGURE 4.** Sugar–phosphate–sugar fragment considered in ref 13 showing the 3′- and 5′-bond cleavages studied (redrawn figure from ref 13).

electron affinity (EA) of the nitrogen radical generated by cleaving this bond].

In 2004, the Märk group showed<sup>10</sup> that the yield for the loss of H atoms (both  $N_1$  and  $N_3$ ) from cytosine and thymine (to produce the corresponding base anions) peaked for electron energies near 1.1–1.5 eV. This suggests that base  $\pi^*$  orbital attachment is likely involved because some of these  $\pi^*$  orbitals have energies in this range (see Figure 1). Also in 2004, the Illenberger group showed<sup>11</sup> that thymidine fragments to produce a sugar radical and thymine anion when exposed to electrons having energies as low as 3 eV, and the Sanche group<sup>12</sup> also in 2004 studied cleavage of the thymine–sugar N–C bond in thymidine but with higher energy electrons.

Finally, the Sanche group has considered<sup>13</sup> the possibility that low-energy electrons can attach to the P=O  $\pi^*$  orbital of a phosphate group and produce cleavage of either the 3′ or 5′ sugar–phosphate C–O  $\sigma$  bond (see Figure 4).

The above body of data suggests that DNA bases can attach electrons in the 1–3 eV range and that cleavage of some of the covalent bonds of bases can result. The most likely attachment sites are the base  $\pi^*$  and phosphate P=O  $\pi^*$  orbitals, and the bonds that had been suggested to cleave include base N–H bonds, the  $N_1$ –C thymine–sugar bond, and phosphate–sugar 3′ and 5′ O–C bonds. We, therefore decided to (i) consider electron attachment to either base  $\pi^*$  or phosphate P=O  $\pi^*$  orbitals to form shape-resonance anions and (ii) determine the energy barriers (if any) needed to cleave base N–H, base–sugar  $N_1$ –C, and sugar–phosphate C–O bonds. Our efforts along these lines form the focus of the remainder of this Account.

### 3. Which Bonds Are Broken and Why?

**3.1. Our DNA Fragments.** In each of our studies, we examined a fragment of DNA using *ab initio* electronic structure methods to determine which bond(s) would be

**FIGURE 5.** Two of the DNA fragments studied in refs 2–6 (see the text for an explanation).

most susceptible to cleavage when an electron is attached to a low-energy base  $\pi^*$  orbital or a P=O  $\pi^*$  orbital. The fragments included (a) the cytosine (C)–sugar–phosphate fragment shown in Figure 5a, (b) an analogous fragment with cytosine replaced by thymine (T), (c) the fragment containing three  $\pi$ -stacked C bases shown in Figure 5b, and (d) the sugar–phosphate–sugar fragment shown in Figure 4.

**3.2. Our Findings.** The most important conclusions of our efforts<sup>2–6</sup> are that (a) attachment of electrons in the 0.1–2 eV range (into C or T  $\pi^*$  orbitals) to form shape resonances can produce covalent-bond cleavages, (b) a sugar–phosphate C–O  $\sigma$  bond is the bond whose cleavage requires surmounting the lowest barrier, (c) cleavage of base–sugar  $N_1$ –C bonds can also occur (as demonstrated experimentally in refs 11 and 12), but this requires surmounting a larger barrier than for the sugar–phosphate C–O bond, (d) cleavage of base  $N_3$ –H bonds can occur<sup>14</sup> (as demonstrated experimentally in refs 9 and 10),

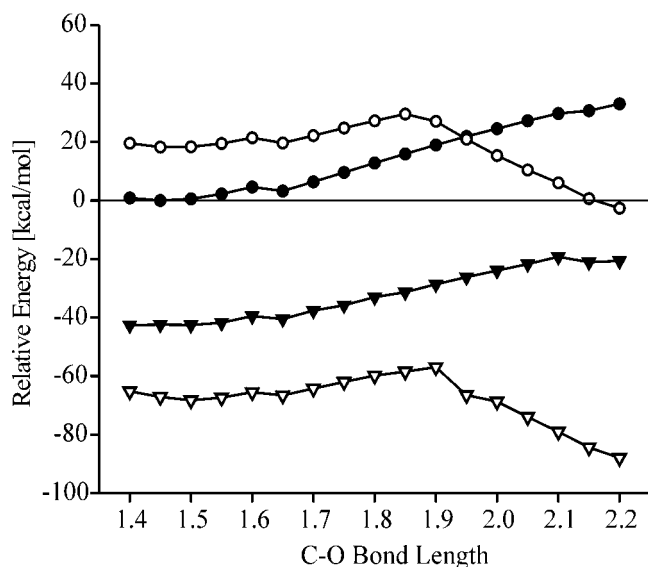


**FIGURE 6.** Energies of the neutral (● and ▼) and cytosine  $\pi^*$ -attached anionic (○ and ▽) cytosine–sugar–phosphate DNA fragment of Figure 5a versus the sugar–phosphate C–O bond length (in angstroms) in the absence of any solvation (top two plots) and with the solvation characterized by the dielectric constant  $\epsilon = 78$  (bottom two plots) (Figure 2 of ref 2).

but a high barrier must be surmounted to do so, (e) the thermodynamic driving force that causes the sugar–phosphate C–O bond to have the lowest barrier is the huge (ca. 5 eV) EA of the phosphate radical, and (f) electron attachment to the P=O  $\pi^*$  orbital requires electrons of higher energy (>2 eV) than for attachment to base  $\pi^*$  orbitals.

### 3.3. Mechanism for C–O, $N_1$ –C, and N–H Cleavage.

To understand how electrons having kinetic energies of 0.1–2 eV can fragment a 4 eV strong C–O  $\sigma$ , we show in Figure 6 energy profiles for the neutral and electron-attached cytosine–sugar–phosphate fragment as functions of the sugar–phosphate C–O bond. The general shapes and characteristics of these plots are characteristic of what we found for all of the bonds studied in refs 2–6 (except, of course, the energy barriers vary among the bond types).

Let us focus on the top two plots in Figure 6, which relate to the fragment shown in Figure 5a in the absence of any solvation (as appropriate to the dry-DNA experiments of ref 7). The first thing to note is that the electron-attached anion lies ca. 1 eV above the energy of the neutral fragment at the equilibrium C–O bond length of the neutral (near 1.45 Å). This reflects the fact that it is endothermic by ca. 1 eV to place an electron into this cytosine  $\pi^*$  orbital to form the shape resonance. The second issue to understand is what causes the profile of the anion to have a barrier, while the profile of the neutral fragment rises monotonically (eventually producing homolytic cleavage products at larger  $R$ ), and what determines how steeply the anion curves fall at large  $R$ . Understanding the origin of the shape of the anion curve lies at the heart of understanding our proposed mechanism of SSB formation; therefore, let us now carefully explain the key ingredients.

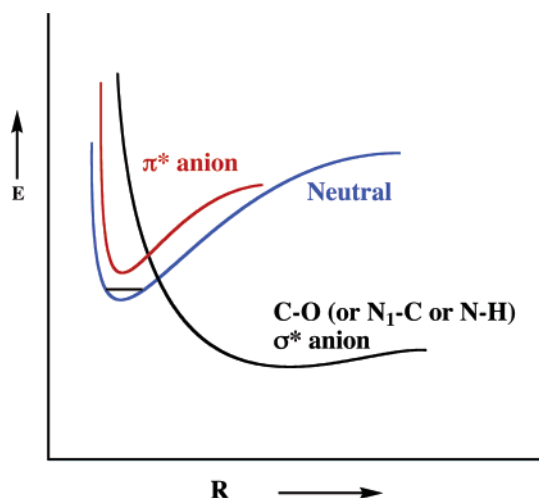


**FIGURE 7.** Qualitative depictions of how the energies of a neutral DNA fragment, a fragment with an electron in a base  $\pi^*$  orbital, and a fragment with an electron in a (C–O,  $N_1$ –C, or N–H)  $\sigma^*$  orbital vary as the C–O,  $N_1$ –C, or N–H bond is elongated.

In Figure 7, we show a qualitative depiction of three so-called diabatic energy profiles that arise in describing cleavage of the sugar–phosphate C–O  $\sigma$  bond (as well as the  $N_1$ –C or N–H bond). The curve labeled neutral shows how the energy varies as any of these  $\sigma$  bonds are elongated in the absence of an attached electron and is a depiction of the homolytic cleavage of the corresponding  $\sigma$  bond.

The curve labeled  $\pi^*$  anion shows how the energy of the DNA fragment varies as the  $\sigma$  bond is elongated if the attached electron is constrained to remain in the  $\pi^*$  orbital. We can effect such a constraint when carrying out our calculations by insisting that the orbital occupation of the appropriate  $\pi^*$  orbital is unity; this is how one constructs these diabatic potential energy profiles. Finally, the curve labeled  $\sigma^*$  anion shows how the energy of the DNA fragment varies if the attached electron is placed into the C–O,  $N_1$ –C, or N–H  $\sigma^*$  orbital.

What do the three energy profiles in Figure 7 have to do with the two profiles shown in the top of Figure 6? The curve labeled neutral in Figure 7 corresponds directly to that given in the ● in Figure 6; both detail the homolytic cleavage of a  $\sigma$  bond. The curve shown by ○ in Figure 6 arises from configuration interaction (CI) between the diabatic  $\pi^*$  anion and  $\sigma^*$  anion curves of Figure 7. The true lowest-energy electron-attached (anion) state in Figure 6 has dominant  $\pi^*$  character for  $R$  ranging up to ca. 1.89 Å and dominant  $\sigma^*$  character for  $R$  greater than ca. 2.0 Å. That is, the  $\pi^*$  and  $\sigma^*$  anion states whose diabatic energy profiles are shown in Figure 7 mix or combine to form the true (adiabatic) electron-attached state whose energy profile is shown in ○ in Figure 6.

This CI mixing is what allows the electron to migrate from the base (or P=O)  $\pi^*$  orbital, where it initially attaches in the electron–DNA collision, to the C–O,  $N_1$ –C, or N–H  $\sigma^*$  orbital. Once the electron occupies the  $\sigma^*$  orbital, cleavage of the corresponding  $\sigma$  bond is prompt because the energy profile of the  $\sigma^*$  anion state is repulsive.<sup>15</sup> To illustrate the evolution of the nature of the

**FIGURE 8.** Singly occupied molecular orbital of cytosine–sugar–phosphate (left) when the attached electron is dominantly in the base  $\pi^*$  orbital (top) or dominantly on the sugar–phosphate  $\sigma^*$  orbital (bottom) and of sugar–phosphate–sugar (middle and right) when the electron is in the P=O  $\pi^*$  orbital (bottom) or in the sugar–phosphate 3' (right top) or 5' (middle top)  $\sigma^*$  orbital.

anion as these  $\sigma$  bonds move, we show in Figure 8 the adiabatic state of the anion as the sugar–phosphate C–O bond is elongated in either a base–sugar–phosphate fragment or a sugar–phosphate–sugar fragment.

We should note that our perspectives on mechanistic issues surrounding how electrons cause these  $\sigma$  bonds to break in DNA have evolved between 2002 when our first paper<sup>2</sup> appeared and the present. This evolution arose as our simulations uncovered new information and through close collaboration with experimentalists who have been studying electron–molecule interactions.

What then happens when an electron having 0.1–2 eV of energy strikes DNA to cause a bond cleavage? First, the electron must attach, and it is to the base  $\pi^*$  or phosphate P=O  $\pi^*$  orbitals that attachment can occur in this energy range. Our studies do not address the dynamics of this electron-attachment process. We have only established the energies of the base  $\pi^*$  and phosphate P=O  $\pi^*$  anion states and obtained the corresponding  $\pi^*$  orbitals in our work; we have also established the energies and orbitals of the C–O, N–C, or N–H  $\sigma^*$  anion states. We carry out such ab initio calculations at a range of C–O (or N–C or N–H) distances to generate neutral,  $\pi^*$ , and  $\sigma^*$  energy profiles such as shown in Figures 6 and 7. Because the anion states are metastable rather than electronically stable, we have had to use special techniques in which we artificially stabilize the anion states by increasing the nuclear charges (by fractional amounts  $\delta q$ ) of the atoms over which the attached electron is delocalized. Computing the anion–neutral energy gap as a function of  $\delta q$  and extrapolating these energies to  $\delta q \rightarrow 0$ , we arrive at our

prediction of the energy of the metastable anion. Details on this charge-stabilization technique are given in ref 3, but it is important to note that it provides only an estimate of the centroid energy of the anion. Because such states are metastable, their states are Heisenberg-broadened; therefore, their energies must be characterized by a centroid and a width. Typical widths for  $\pi^*$  shape resonances are 0.5 eV and  $>1$  eV for  $\sigma^*$  shape resonances.

Having used the above methods to compute, for example, the energy profiles in Figure 6, we suggest that there are two ways that the bond cleavage might occur. First and as we described in our work to date,<sup>2–6,14</sup> thermal vibrational motions cause the C–O bond to vibrate about its equilibrium bond length of ca. 1.45 Å. If an electron having kinetic energy near 1 eV strikes the cytosine moiety when the C–O bond length is shorter than ca. 1.8 Å, it can enter one of the  $\pi^*$  orbitals of this base and form the metastable  $\pi^*$  state. Then, if the C–O bond has enough time (the electron may detach in ca.  $10^{1-4}$  s) to move to 1.85 Å, the attached electron can adiabatically migrate (as illustrated in Figure 8) from the  $\pi^*$  orbital to the sugar–phosphate C–O  $\sigma^*$  orbital, after which the C–O bond promptly breaks. Alternatively, the C–O bond may already be elongated (by vibrational motion) to near 1.85 Å when the incident electron strikes and attaches to form a mixed  $\pi^*/\sigma^*$  anion. In both cases, the anion lies ca. 1 eV above the neutral and the energy required to stretch the C–O bond is the same because the neutral and anion surfaces are nearly parallel along the C–O coordinate in this range. Analogous steps were predicted to occur when an electron attaches to a base  $\pi^*$  orbital and a base–sugar N<sub>1</sub>–C or

base N–H bond is broken or when an electron attaches to a P=O  $\pi^*$  orbital and a sugar–phosphate (3' or 5') bond is cleaved.

Another interesting possibility but one that experiments have not yet been able to probe is that thermal vibrational excitation of the neutral may be sufficient to access C–O distances of 1.90–1.95 Å. Then, an electron with energy below 1 eV (near 1.9 Å) could attach, or (near 1.95 Å) exothermic electron attachment might take place (e.g., by exciting other vibrational modes) to form an anion state that subsequently undergoes C–O bond cleavage. Although this mechanistic alternative would require more vibrational excitation of the C–O bond and could involve lower energy electrons, present experimental limitations (e.g., electron energy range limits and control of C–O vibrational populations) do not allow us to yet test its validity.

**3.4. Estimating Rates.** To illustrate how we estimated the rates of C–O, N<sub>1</sub>–C, and N–H bond cleavage based on the first mechanistic model discussed above, let us again use the data shown in Figure 6. We obtain rates by multiplying the C–O vibrational frequency (ca.  $10^{13}$  s<sup>-1</sup>) by the equilibrium Boltzmann probability

$$P = \exp(-E^*/kT)/q \quad (1)$$

that the C–O bond is stretched enough (either before or after electron attachment) to reach the barrier (of height  $E^*$ ) on the energy profile of the anion near  $R = 1.85$  Å in Figure 6. The symbol  $q$  in eq 1 is the vibrational partition function for the C–O stretching mode. The barrier heights  $E^*$  found<sup>2–6</sup> when electrons are attached to cytosine or thymine ranged from 0.2 to 1 eV, depending upon the energy, within the Heisenberg broadened shape resonance, the electron possesses. As a result, the estimated  $T = 298$  K (as in ref 7) C–O bond cleavage rates range from  $10^{10}$  to  $10^{-4}$  s<sup>-1</sup>. Because the autodetachment rate of a  $\pi^*$  shape resonance is expected to be near  $10^{14}$  s<sup>-1</sup>, our bond cleavage estimates suggested that at most 1 in  $10^4$  nascent  $\pi^*$  anions will undergo C–O bond rupture. We should emphasize that uncertainties of 0.1–0.2 eV in our computed barrier heights exist. Therefore, it is probably best to conclude that rates of passage over barriers on the  $\pi^*/\sigma^*$  surfaces may be consistent with observed strand-break yields, but uncertainties in the energy barriers do not allow us to make quantitative such comparisons.

**3.5. Which Bonds Cleave?** To predict the relative rates at which sugar–phosphate C–O, base–sugar N<sub>1</sub>–C, and base N–H bond break, we needed to compute the energy profiles for all of these bonds to obtain data analogous to that shown in Figure 6. In refs 2–6, we did so, and an example of another profile is shown in Figure 9 for attachment of a 0.8 eV electron to a  $\pi^*$  orbital in a thymine–sugar–phosphate model system to cleave the N<sub>1</sub>–C bond.

When Figures 6 and 9 are compared, it is clear that the barrier to cleavage of the sugar–phosphate C–O bond is considerably lower than that for N<sub>1</sub>–C bond cleavage. Likewise, we found<sup>14</sup> that the barrier for breaking a base N<sub>3</sub>–H bond is higher than the C–O barrier. It is through

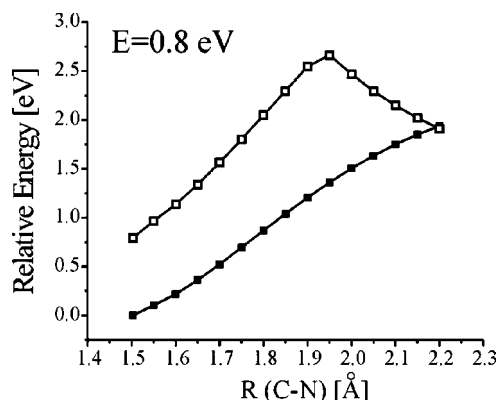


**FIGURE 9.** Energy profile for the neutral (■) and anion (□) thymine–sugar–phosphate unit as a function of the thymine–sugar N<sub>1</sub>–C bond length (Figure 7 of ref 5).

such barrier-height determinations that we were able to predict which bonds would break at the highest rates in DNA. As a result, we predicted that it is the sugar–phosphate C–O bonds that have the lowest barriers to cleavage and thus are expected to cleave at the highest rates in DNA. Thus, we suggested that SSBs induced by electrons in the 0.1–2 eV range that attach to form shape-resonance anions arise (predominantly) from cleaving backbone sugar–phosphate C–O  $\sigma$  bonds.

Why is it that the barrier toward cleaving the sugar–phosphate C–O bond is the lowest? To understand the answer, let us return to Figure 7. A primary difference among cleaving sugar–phosphate C–O, base–sugar N<sub>1</sub>–C, and base N<sub>3</sub>–H bonds arises in the electron affinities of the radical species generated upon such bond fragmentation. The oxygen site of the phosphate radical generated when the C–O bond breaks has an EA of ca. 5 eV, whereas the nitrogen-centered radicals generated in N<sub>1</sub>–C or N–H bond cleavage have EAs of only ca. 3.5 eV. As a result, the large- $R$  asymptote of the  $\sigma^*$  anion curve in Figure 7 lies much lower in the C–O bond cleavage case than in the other cases. Hence, it is the huge EA of the phosphate site that provides the thermodynamic driving force for breaking the C–O bond and is the reason that the  $\sigma^*$  anion branch of the electron-attached curve in Figure 6 descends steeply at large  $R$  and crosses the  $\pi^*$  anion branch with such a low barrier.

### 3.6. Do the Electrons Attach to Phosphate $\pi^*$ Orbitals?

As mentioned earlier, we also considered the sugar–phosphate–sugar fragment shown in Figure 4. We did this not only to consider the barriers to breaking a 3' or 5' sugar–phosphate C–O bond but also to determine what kinetic energy an electron would have to have to attach to the phosphate P=O  $\pi^*$  orbital. In Figure 10, we display the neutral, P=O  $\pi^*$  anion, and 3' and 5' C–O  $\sigma^*$  anion energy profiles that we obtained using the charge-stabilization method<sup>3</sup> discussed earlier.

These data show that vertical attachment of an electron to a P=O  $\pi^*$  orbital requires an electron of kinetic energy near 2 eV. Because the DNA bases have  $\pi^*$  orbitals (see Figure 2) in the 0.1–2 eV range, we concluded that electrons below ca. 2 eV probably attach only to base  $\pi^*$

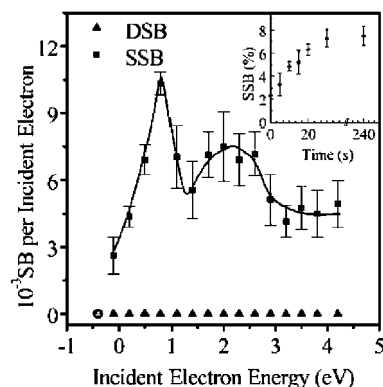


**FIGURE 11.** Yield of DNA-strand breaks as a function of the electron kinetic energy showing SSBs occurring in the 0.1–2 eV range (Figure 1 of ref 16).

	C	p	G	p	T	p	A
Phosphate	0.23	0.29	0.11	0.19	0.19	0.20	
base release	0.27	0		0.12		0.35	
total	0.50	0.40		0.50		0.55	
	G	p	C	p	A	p	T
Phosphate	0.27	0.11	0.22	0.16	0.23	0.31	
base release	0.22	0.03		0.11		0.35	
total	0.49	0.36		0.50		0.66	

**FIGURE 12.** Data (Scheme 1 of ref 17) showing the yields of the sugar–phosphate bond cleavage determined by chemical analysis of the products formed when CGTA and GCAT oligomers were exposed to electrons.

**FIGURE 10.** Energies of the neutral,  $\pi^*$ -attached anion, and  $\sigma^*$ -attached anion as functions of the 3'-C-O (top) and 5'-C-O (bottom) C-O bond lengths (Figure 3 of ref 5).

orbitals, but electrons with energy exceeding 2 eV could attach either to base  $\pi^*$  or to P=O  $\pi^*$  orbitals.

In summary, our series of theoretical simulations allowed us to predict that, for electrons in the 0.1–2 eV range, SSBs are most likely be formed when (a) an electron enters a low-lying  $\pi^*$  orbital of a DNA base to form a shape resonance, after which (b) a through-bond electron-transfer event occurs if the sugar–phosphate C–O  $\sigma$  bond is elongated (e.g., through normal thermally activated vibrational motions) to near 1.85 Å, allowing for a barrier to be surmounted and  $\pi^*/\sigma^*$  configuration interaction to take place, (c) producing a  $\sigma^*$ -attached anion that promptly fragments to yield a carbon radical and a (very stable) phosphate-site anion.

For electrons above 2 eV, SSB formation can also involve attachment to P=O  $\pi^*$  orbitals followed by passing over a barrier (see Figure 10) to cleave the 3' or 5' sugar–phosphate C–O bond. Finally, the primary reason underlying the preference for sugar–phosphate C–O bond cleavage is the huge EA of the phosphate radical.

#### 4. Experimental Verifications

After our studies suggesting that shape resonances could induce sugar–phosphate C–O strand breaks in DNA, new measurements<sup>16</sup> were carried out in a collaboration of the

Sanche and Burrow groups at even lower electron kinetic energies and strand breaks were indeed observed as Figure 11 illustrates.

This shows that we were correct in predicting that shape resonances induce SSBs.

In ref 16, it was also shown that the shape of the strand-break yield plot of Figure 11 could be simulated by superposing the energy dependence of the electron attachment cross-sections of the four DNA bases (assuming an equal distribution of the four bases in the DNA sample used in ref 16). This observation provides further evidence supporting our claim that it is primarily to the base  $\pi^*$  and not the phosphate P=O  $\pi^*$  orbitals that attachment occurs.

Finally, a more recent experimental result of Sanche<sup>17</sup> offers support to our prediction that it is primarily the backbone sugar–phosphate C–O bonds that are cleaved in shape-resonance-induced SSBs. In these experiments, oligonucleotide tetramers (CGTA and GCTA) were exposed to electrons after which the chemical identities of the products of irradiation were determined by high-pressure liquid chromatography. These experiments (see Figure 12) show primarily cleavage of the phosphodiester (sugar–

phosphate C–O) bonds in line with our prediction, although there also appears to be some cleavage of the base–sugar N<sub>1</sub>–C bond.

## 5. Summary

In this Account, we used results from several of our recent studies to illustrate how we have been able to propose mechanisms by which very low-energy (0.1–2 eV) free electrons attach to dry DNA to cause strong (ca. 4 eV) covalent bonds to break. The primary conclusions of this body of work have been that (i) attachment to base  $\pi^*$  orbitals to form shape resonances in the 0.1–2 eV energy range most likely results in cleavage of sugar–phosphate C–O  $\sigma$  bonds; the base  $\pi^*$  orbitals serve as the “antennas” to which the low-energy electrons attach, (ii) attachment to P=O  $\pi^*$  orbitals may contribute to SSB formation but only for electrons having energies in excess of 2 eV, (iii) the thermodynamic driving force that favors sugar–phosphate C–O bond rupture over base–sugar N<sub>1</sub>–C or base N–H bond cleavage is the large EA of the phosphate radical, and (iv) the rates of C–O bond cleavage are determined by the rate at which an energy barrier on the potential surface of the anion is surmounted.

After our works in which the above predictions were offered, very recent experiments have appeared in which (i) convincing evidence<sup>16</sup> is given in support of our claim that 0.1–2 eV electrons attach to base  $\pi^*$  orbitals rather than to P=O  $\pi^*$  orbitals and (ii) chemical analysis of the products of strand breaks shows<sup>17</sup> that it is indeed primarily the sugar–phosphate C–O bonds that break.

One aspect of the mechanism that we predicted for SSB formation by very low-energy electrons might be surprising to some readers. In particular, one might wonder why the distant sugar–phosphate C–O bond breaks when both experiment and theory have shown that the base N–H and base–sugar N<sub>1</sub>–C bonds can also break. After all, the latter two bonds are much closer to the base  $\pi^*$  orbital to which the electron is believed to initially attach. The answer to this question is that the barrier to C–O bond cleavage is lower than that for N<sub>1</sub>–C or N–H cleavage (because of the much higher EA of the phosphate radical).

We also note that, for the electron to migrate to the C–O  $\sigma^*$  orbital, it does not have to first enter the N<sub>1</sub>–C  $\sigma^*$  orbital (and hence potentially break this N<sub>1</sub>–C bond); the N<sub>1</sub>–C  $\sigma^*$  orbital simply has to assist the migration of the electron from the base and onto the sugar on its way to the sugar–phosphate linkage. This kind of through-bond electron transfer to a distant leaving group of high EA occurs in many contexts in chemistry and biology. An excellent example is offered by an collaboration from the Jordan and Burrow groups<sup>18</sup> who attached electrons to olefinic  $\pi^*$  orbitals separated from a C–Cl bond by rigid aliphatic spacer groups. They observed Cl<sup>–</sup> anion formation after  $\pi^*$ -orbital attachment, and they argued that the through-bond  $\pi^*/\sigma^*$  orbital coupling is what produces the Cl<sup>–</sup> ions.

Before closing, it is worth noting that an excellent review appeared recently<sup>19</sup> covering much of the recent history of studies related to electron-induced strand breaks in DNA. In particular, the situation surrounding

damage induced by electrons having energies higher than considered here is very nicely reviewed. Work on electron-induced bond cleavage in DNA bases (where H atom elimination and base radical anion formation occurs), in base–sugar units (where cleavage of the bond connecting the base to the sugar occurs), and in sugar–phosphate units (where the sugar–phosphate C–O bond cleaves) is overviewed. In addition, the potential role of dipole-bound states in the initial electron attachment is also discussed.

*Support of the National Science Foundation through Grant CHE 0240387 is appreciated as is significant computer time provided by the Center for High Performance Computing at the University of Utah.*

## References

- (1) Connell, P.; Kron, S.; Weichselbaum, R. *DNA Repair* **2004**, *3*, 1245–1251.
- (2) Barrios, R.; Skurski, P.; Simons, J. Mechanism for Damage to DNA by Low-Energy Electrons. *J. Phys. Chem. B* **2002**, *106*, 7991–7994.
- (3) Berdys, J.; Anusiewicz, I.; Skurski, P.; Simons, J. Damage to Model DNA Fragments from Very Low-Energy (<1 eV) Electrons. *J. Am. Chem. Soc.* **2004**, *126*, 6441–6447.
- (4) Berdys, J.; Anusiewicz, I. P.; Simons, J. Theoretical Study of Damage to DNA by 0.2–1.5 eV Electrons Attached to Cytosine. *J. Phys. Chem. A* **2004**, *108*, 2999–3005.
- (5) Anusiewicz, I.; Berdys, J.; Sobczyk, M.; Skurski, P.; Simons, J. Effects of Base  $\pi$ -Stacking on Damage to DNA by Low-Energy Electrons. *J. Phys. Chem. A* **2004**, *108*, 11381–11387.
- (6) Berdys, J.; Skurski, P.; Simons, J. Damage to Model DNA Fragments by 0.25–1.0 eV Electrons Attached to a Thymine  $\pi^*$  Orbital. *J. Phys. Chem. B* **2004**, *108*, 5800–5805.
- (7) Boudaiffa, B.; Cloutier, P.; Hunting, D.; Huels, M. A.; Sanche, L. Resonant Formation of DNA Strand Breaks by Low-Energy (3 to 20 eV) Electrons. *Science* **2000**, *287*, 1658–1662.
- (8) Aflatooni, K.; Gallup, G. A.; Burrow, P. D. Electron Attachment Energies of the DNA Bases. *J. Phys. Chem. A* **1998**, *102*, 6205–6207.
- (9) Ptasinska, S.; Denifl, S.; Grill, V.; Märk, T. D.; Scheier, P.; Gohlke, S.; Huels, M. A.; Illenberger, E. Bond-Selective H<sup>–</sup> Ion Abstraction from Thymine. *Angew. Chem., Int. Ed.* **2005**, *44*, 1647–1650. (b) Ptasinska, S.; Denifl, S.; Grill, V.; Märk, T. D.; Illenberger, E.; Scheier, P. Bond- and Site-Selective Loss of H<sup>–</sup> from Pyrimidine Bases. *Phys. Rev. Lett.* **2005**, *95*, 093201-1–093201-2.
- (10) Denifl, S.; Ptasinska, S.; Probst, M.; Hrusak, J.; Scheier, P.; Märk, T. D. Electron Attachment to the Gas-Phase DNA Bases Cytosine and Thymine. *J. Phys. Chem. A* **2004**, *108*, 6562–6569.
- (11) Abdoul-Carime, H.; Gohlke, S.; Fischbach, E.; Scheinke, J.; Illenberger, E. Thymine Excision from DNA by Subexcitation Electrons. *Chem. Phys. Lett.* **2004**, *387*, 267–270.
- (12) Zheng, Y.; Cloutier, P.; Hunting, D. J.; Wagner, J. R.; Sanche, L. Glycosidic Bond Cleavage of Thymidine by Low-Energy Electrons. *J. Am. Chem. Soc.* **2004**, *126*, 1002–1003.
- (13) Li, X.; Sevilla, M.; Sanche, L. Density Functional Theory Studies of Electron Interaction with DNA: Can Zero eV Electrons Induce Strand Breaks? *J. Am. Chem. Soc.* **2003**, *125*, 13668–13669.
- (14) Théodore, M.; Sobczyk, M.; Simons, J. Cleavage of Thymine N<sub>3</sub>–H Bonds by Low-Energy Electrons Attached to Base  $\pi^*$  Orbitals. *Chem. Phys.* **2006**, in press.
- (15) This is true except for a shallow ion–molecule complex between the departing anion and radical fragments.
- (16) Martin, F.; Burrow, P. D.; Cai, Z.; Cloutier, P.; Hunting, D.; Sanche, L. DNA Strand Breaks Induced by 0–4 eV Electrons: The Role of Shape Resonances. *Phys. Rev. Lett.* **2004**, *93*, 068101-1–068101-4.
- (17) Zheng, Y.; Cloutier, P.; Hunting, D.; Sanche, L.; Wagner, J. R. Chemical Basis of DNA Sugar–Phosphate Cleavage by Low-Energy Electrons. *J. Am. Chem. Soc.* **2005**, *127*, 16592–16598. (b) Zheng, Y.; Cloutier, P.; Hunting, D.; Wagner, J. R.; Sanche, L. Phosphodiester and N-glycosidic bond cleavage in DNA induced by 4–15 eV electrons. *J. Chem. Phys.* **2006**, *124*, 064710-1–064710-9.
- (18) Pearl, D. M.; Burrow, P. D.; Nash, J. J.; Morrison, H.; Nachtigallova, D.; Jordan, K. D. Dissociative Attachment as a Probe of the Distance Dependence of Intramolecular Electron Transfer. *J. Phys. Chem.* **1995**, *99*, 12379–12381.
- (19) Sanche, L. Low Energy Electron-Driven Damage in Biomolecules. *Eur. Phys. J. D* **2005**, *35*, 367–390.

AR0680769